[6] A. Beyer and I. Wolff, "The solution of the earthed fin line with finite metallization thickness," in *IEEE MTT-S Symp. Dig.*, 1980, pp. 258–260.
[7] P. J. B. Clarricoats, *Microwave Ferrites*. London: Chapman & Hall, 1961.
[8] A. Beyer and I. Wolff, "Calculation of the transmission properties of inhomogeneous fin lines," in *Proc. 10th European Microwave Conf., 1980*, pp. 322–326.
[9] L. Courtois and M. De Vecchis, "A new class of nonreciprocal components using slot line," *IEEE Trans. Microwave Theory Tech.*, vol. MTT-23, pp. 511–516, June 1975.
[10] A. G. Gurevich, *Ferrites at Microwave Frequencies*. New York: Consultants Bureau, 1963.

Adalbert Beyer, photograph and biography not available at the time of publication.

Klaus Solbach (M'80), for a photograph and biography please see page 77 of the January issue of this TRANSACTIONS.

Integrated Circuit Compatible Surface Acoustic Wave Devices on Gallium Arsenide

THOMAS W. GRUDKOWSKI, MEMBER, IEEE, GARY K. MONTRESS, MEMBER, IEEE, MEYER GILDEN, MEMBER, IEEE, AND JAMES F. BLACK, MEMBER, IEEE

Abstract—**Improvements in gallium arsenide materials technology have led to the rapid development of GaAs MIC [1], CCD [2], and digital IC [3] technologies in the last several years. In this paper we consider the additional capabilities afforded by the inherent piezoelectric properties of GaAs [4]. The primary emphasis of the work is on surface acoustic wave (SAW) device configurations using MESFET and Schottky-barrier diode fabrication techniques which are compatible with the eventual monolithic integration of electronic devices on the same substrate. The GaAs SAW technology described here provides a means for achieving electronically variable delay, high-Q resonator structures for VHF/UHF oscillator frequency control, and real-time signal processing operations such as convolution and correlation. Prototype device designs and performance are described, including two-port GaAs SAW resonators with Q's as large as 13 000 at 118 MHz and a programmable GaAs SAW PSK correlator capable of signal correlation at 10-MHz chip rates. Further GaAs SAW device development required for increasing the operating frequency range to 500 MHz and processing bandwidth to 100 MHz is indicated.**

I. INTRODUCTION

THE CAPABILITIES of GaAs technology for meeting the advanced requirements of analog and digital system designs are increasingly evident. These capabilities are based for the most part on the superior semiconducting properties of GaAs as compared to silicon. In particular, the larger electron mobility and wider bandgap of GaAs provide the means for achieving higher device operating frequency, speed, and temperature. In addition, the availability of semi-insulating GaAs substrate material makes the extension of device operating frequency into the microwave region possible and allows for great flexibility in the techniques used for device interconnection.

In this paper we describe some of the fundamental aspects of SAW device operation on GaAs as well as several new and promising device developments. By using an n-type semiconducting layer on a semi-insulating GaAs substrate one may combine the piezoelectric and semiconducting properties either indirectly or directly. For example, these properties may be treated separately by fabricating SAW delay lines, resonators, or filters on the semi-insulating substrate and combining these components with electronic components fabricated on an adjacent epitaxial or ion-implanted semiconducting layer using thin film interconnects. Alternatively, the SAW/electronics coupling may be performed directly through acoustoelectric interaction of the SAW electric field with the charge carriers or the potential distribution within a diode or FET. Either approach leads to monolithic device designs which may reduce circuit size, power consumption, and cost as compared to hybrid approaches and also extends the capabilities and design options available for GaAs IC development.

The SAW device configurations described here typically operate within the 100–200-MHz frequency range although extension to 1 GHz is feasible, limited primarily by increasing propagation loss [5]. The use of a nominal ⟨001⟩ oriented substrate is consistent with that used for GaAs IC

Manuscript received April 13, 1981; revised August 5, 1981. This work was supported in part by USAERADCOM under Contract DAAK20-79-C-0263 and by the Rome Air Development Center under Contract F19628-79-C-0056.

The authors are with United Technologies Research Center, East Hartford, CT 06108.

0018-9480/81/1200-1348$00.75 ©1981 IEEE

development. SAW propagation along a (110) or equivalent direction is preferred because the piezoelectric coupling to the surfaces waves is maximum for this substrate orientation.

In several ways, the SAW properties of ⟨001⟩, (110) oriented GaAs and those of a common SAW substrate, ST-X quartz, are similar. The SAW velocities of 2868 m/s for GaAs and 3157 m/s for ST-X quartz are quite close, while the piezoelectric coupling strength, $\Delta v/v = 0.00036$, for GaAs is only 38 percent less than the value found for ST-X quartz. The most pronounced difference between the two piezoelectric materials is that the linear temperature coefficient of phase delay, TCD, is approximately +52 ppm/°C for GaAs, and zero for ST-X quartz at 25°C. However, a temperature compensation technique has been demonstrated showing that a zero linear TCD on GaAs can be achieved by using thin film overlays which are deposited onto the substrate [6], [7]. Alternatively, depending upon the application, other techniques (e.g., temperature compensation of an oscillator using electronic techniques) may be used to achieve temperature compensated device operation.

After first briefly summarizing methods used to excite surface waves for narrow-bandwidth and broad-bandwidth applications, the remainder of the paper concentrates on device structures for frequency control and signal processing applications. These structures include voltage tunable SAW phase shifters, high-Q fixed and tunable SAW resonators, tunable GaAs SAW oscillators, monolithic SAW convolvers, and asynchronous SAW correlator/programmable matched filters.

II. Transduction Techniques

Interdigital transducers fabricated on semi-insulating GaAs make use of the available piezoelectric coupling and can be designed using standard methods by treating the substrate as an insulator [8], [9]. Typically, one-port transducer conversion losses of 22 dB untuned and 11 dB tuned, and fractional transducer bandwidths of 5–10 percent are readily achieved. However, when using semiconducting material, the effect of the mobile charge carriers is to short out the piezoelectric fields of the wave and also the exciting fields of the transducer. In order to overcome these problems, the transducer electrodes are fabricated as Schottky barriers. The basic transducer design is shown schematically in Fig. 1(a). When a negative dc bias voltage is applied as shown, the mobile charge carriers beneath the transducers are depleted and the transducer operates as if it were on the equivalent insulating GaAs substrate. Fig. 1(b) and (c) illustrate the effect of reverse dc bias voltage on transducer impedance and delay line (two-port) insertion loss, respectively. For these measurements, 35 wavelength long transducers fabricated on a 1.75-μm thick epitaxial layer with a doping concentration of $n = 9 \times 10^{15}/\text{cm}^3$ were used. The transducer aperture was 1.0 mm. It is evident that a 35-dB decrease in delay line insertion loss is achieved with the application of a dc bias voltage of −20 V, as compared to the insertion loss with no reverse

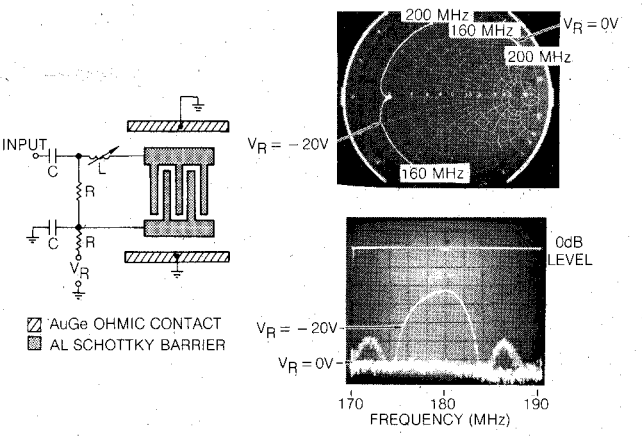

Fig. 1. Schottky-barrier interdigital electrode transducer design and performance on epitaxial GaAs. (a) Transducer structure with $R = 10$ kΩ, $C = 1.0$ μF, and $L \cong 195$ nH. Transducer synchronous frequency is approximately 180 MHz. (b) Swept transducer input impedance for $V_R = 0$ V and −20 V. (c) Swept two-port delay line insertion loss for $V_R = 0$ V and −20 V.

bias voltage applied. This bias voltage is exactly that required to completely deplete the epitaxial layer beneath the transducer electrodes of all mobile charge carriers. Proportionately larger or smaller reverse dc bias voltages would be required on other epitaxial layers, depending upon their doping and thickness. Transducers fabricated directly on either semi-insulating or epitaxial GaAs substrates are suitable for narrow-bandwidth (≤10 percent) applications such as SAW resonators for oscillator frequency control or moderate processing rate convolvers and correlators. The parasitic series resistance of about 5 Ω shown in Fig. 1(b) is attributable to conductor losses in the aluminum transducer metallization. Typically, parasitic series resistance values in the range of 2–6 Ω have been measured. Using a simple equivalent circuit model for the transducer it is readily shown that this parasitic resistance only contributes 1–3 dB of excess conversion loss [8], [9], which is not a serious problem in most applications.

When fractional bandwidths exceeding about 10 percent with moderate conversion loss are required (e.g., large processing rate convolvers), transducers fabricated on ZnO overlay films may be used, as previously reported for other substrates [10], [11]. The greater piezoelectric coupling strength provided by the ZnO film allows for the design of broader bandwidth transducers for the same level of conversion loss. If even greater fractional bandwidths are required (≥30 percent), alternate design techniques are available although with a sacrifice in ease of fabrication. One such technique, the use of edge-bonded transducers [12]–[14] holds the promise of achieving octave or greater bandwidths with low conversion losses.

III. Frequency Control Devices

A. GaAs SAW Phase Shifters

The use of a Schottky-barrier contact to deplete an epitaxial layer of mobile charge carriers was described previously as a means for eliminating the electric field shorting effect of the carriers beneath the transducer. The

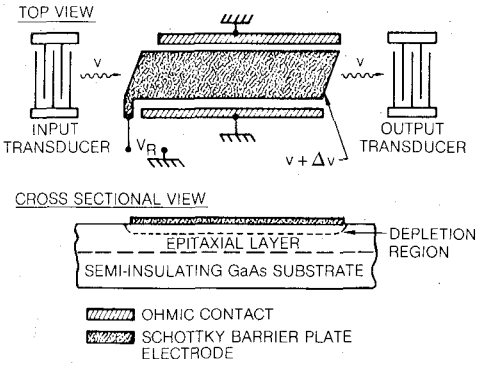

Fig. 2. Top and cross-sectional view of a SAW delay line phase shifter design.

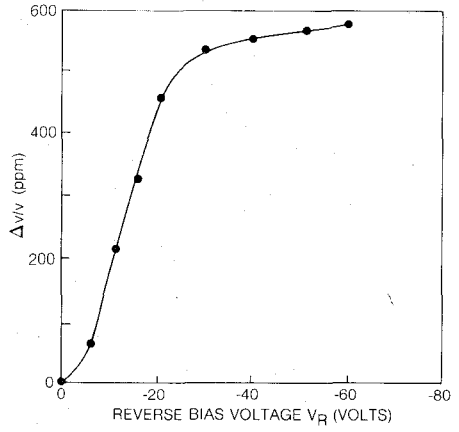

Fig. 3. Measured delay line phase shifter performance. Delay path length is 1 cm, and $f=118$ MHz.

shorting effect within the active layer can also be used to advantage in controlling the SAW velocity between two transducers. As shown schematically in Fig. 2, the degree of shorting may be controlled by varying the depletion depth beneath a Schottky-barrier phase shifting electrode. As the depletion depth is increased with increasing reverse bias, the SAW electric fields within the bulk are gradually restored until an effective insulating condition is reached. The relative velocity change, $\Delta v/v$, available by controlling the free carriers within the bulk of the material is significantly higher than that available when a massless shorting metallic film is placed at the surface alone. For the surface short, $\Delta v/v=0.00036$, whereas a value of $\Delta v/v=0.00093$ is computed for the effective bulk shorting condition relative to the electrode-free insulating crystal [15]. An effective short is produced when the conduction frequency of the material is much greater than the SAW frequency, a condition which is readily achieved in practice.

The change in SAW velocity versus reverse bias voltage produced with an experimental SAW phase shifter is shown in Fig. 3. The epitaxial layer thickness and carrier concentration were 4 μm and $n=10^{15}/\text{cm}^3$, respectively. The phase shifting electrode path length was 1 cm. The maximum velocity change observed, approximately 575 ppm, corresponds to an electronically adjustable phase shift of 85 degrees at 118 MHz. For operation at 200 MHz, a

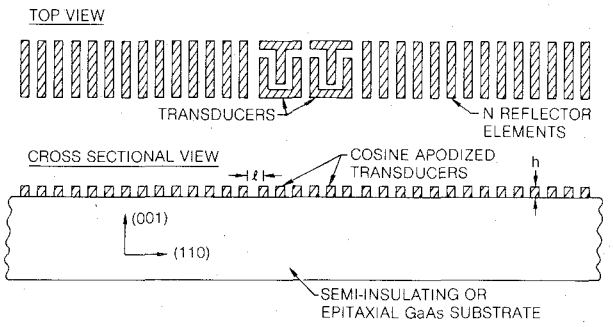

Fig. 4. Top and cross-sectional views showing basic SAW resonator structure and design for the case of metallic reflectors.

90-degree phase shift control range could be achieved for a 0.65-cm long electroded propagation path length. Throughout the voltage tuning range, the variation in SAW propagation loss was less than 0.5 dB for a 1-cm long electrode at a frequency of 118 MHz. The dc power drain of the phase shifter is extremely low because the Schottky barrier electrode is reverse biased.

B. Two-Port GaAs SAW Resonators

The ability to fabricate high-Q SAW resonators on GaAs has potential impact on the construction, in a monolithic form, of stable VHF/UHF oscillators with good short-term stability and low near carrier phase noise. Loaded Q values achieved in air, as measured in a 50-Ω system, for GaAs SAW resonators are 11 500 at 179 MHz and 13 000 at 118 MHz. These Q values are comparable to those achieved for quartz SAW resonator devices, and when coupled with temperature compensation techniques, such as thin film overlays [6], [7], will allow the fabrication of stable fundamental frequency VHF/UHF sources operating in the 100–500-MHz frequency range.

Two-port SAW resonators have been fabricated, initially on semi-insulating GaAs, using both ion-milled groove reflectors and metallic strip reflectors. The metallic strip reflectors, when fabricated as Schottky-barrier contacts, are also of interest for the construction of voltage tunable SAW resonators on epitaxial GaAs substrates. Our initial experiments have been directed at determining the design parameters which affect the resonator response, as has been previously done for quartz [16], [17]. The effects of several of these parameters are described here. While the optimum design iterations have not as yet been experimentally implemented, the results achieved thus far indicate that the material is capable of supporting high Q's, approaching those of quartz at its comparable state of development. When considered for its potential for integrated circuit implementation, the Q's achieved greatly exceed those available using conventional thin film IC techniques [18].

The SAW resonator design used is shown schematically in Fig. 4(a) and (b) for the case of metallic strip reflectors. The transducers are 29 wavelength long, quarter-wavelength electrode designs with 1.0-mm aperture and cosine apodization. The transducer-to-grating separation, l, of 1.75λ has been found to be optimum for metallic strip reflectors

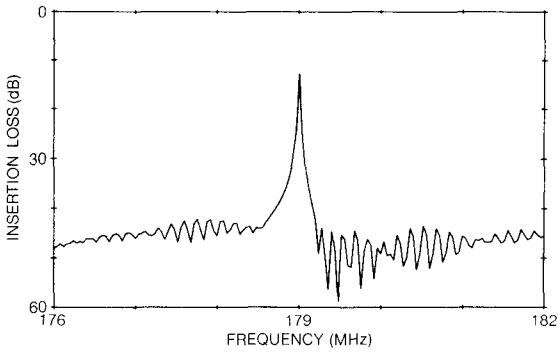

Fig. 5. Typical frequency response (insertion loss) characteristic for a GaAs SAW resonator fabricated on semi-insulating GaAs substrate. The resonant frequency was approximately 179 MHz and the loaded Q was about 9300. The gratings were metallic strip reflectors.

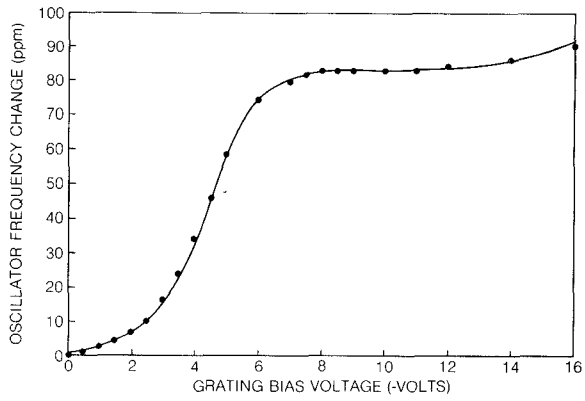

Fig. 6. Frequency tuning characteristics for an oscillator fabricated using a two-port GaAs SAW resonator. The resonator was fabricated on an epitaxial GaAs substrate with Schottky-barrier metallic strip reflectors. Nominal oscillator frequency was approximately 179 MHz and the resonator loaded Q was about 8000.

while a value of 2.00λ is optimum for grooved reflectors. These values are in agreement with designs fabricated on quartz [19]. Fig. 5 shows the measured untuned insertion loss characteristic for a metallic strip reflector device fabricated on semi-insulating GaAs. The resonator was designed with 1000 reflector elements per grating. The overall device size could be reduced considerably if fewer reflector elements were included in the gratings. For the designs used, 600 reflector elements per grating would only reduce the value of Q by 5 percent. This means that the size of a 300-MHz resonator would only be approximately 0.040 in wide by 0.250 in long. These dimensions are completely compatible with present processing technology and electronic device sizes. A chrome/aluminum metallization was used for transducer and metallic strip reflector fabrication, with a 100-Å thick chrome layer beneath a 700-Å thick aluminum metal layer. The untuned insertion loss and Q for the device were about 12 dB and 9300, respectively, comparable to the performance of identically designed devices fabricated on quartz. The reflector step height was approximately $h = 0.01\lambda$. Further design refinements taking into account the effects of grating depth and metallization thickness on SAW velocity, similar to those done for quartz [16], [17], are necessary in order to achieve optimum GaAs SAW resonator performance.

C. Voltage Tunable GaAs SAW Resonator Oscillator

As indicated previously, the resonator reflector gratings may be designed with metallic strip reflectors fabricated using Schottky barrier electrodes on an epitaxial GaAs substrate. This allows for oscillator frequency control when the SAW resonator is incorporated in a feedback oscillator design. The preliminary results described here offer the possibility for developing stable, high-Q SAW controlled VHF/UHF oscillators fabricated on a monolithic GaAs substrate. The use of a GaAs SAW resonator oscillator as a local oscillator is apparent.

A voltage tunable two-port GaAs SAW resonator fabricated on an epitaxial GaAs substrate was used as the frequency controlling element in a feedback oscillator design. The general design of the GaAs SAW resonator followed standard SAW resonator design procedures and is similar to that illustrated in Fig. 4. However, a Schottky-barrier metallization was used to form the resonator metallic strip reflectors and all reflector elements in each grating were connected by a common buss electrode so that a reverse dc bias voltage could be uniformly applied to each grating. Varying the reverse dc bias voltage applied to the reflector gratings changes the effective SAW velocity within the gratings thus allowing electronic oscillator frequency control by varying the transmission phase of the resonator. Because the resonant frequency and transmission phase characteristics track as the grating reverse bias voltage is varied, oscillator frequency (after initial external frequency trimming) is maintained at the resonant frequency of the GaAs SAW resonator.

The frequency tuning range, frequency temperature sensitivity, and short-term stability (Allan variance) for a one second gating time were evaluated for the tunable GaAs SAW resonator oscillator. The oscillator frequency change (ppm) versus dc reverse bias voltage applied to both resonator gratings is shown in Fig. 6. The general behavior of the oscillator tuning characteristic is similar to those found for the delay line phase shifters (Fig. 3) described previously. The maximum total frequency tuning range for the oscillator was approximately 80 ppm, for a total grating bias voltage change from 0 to −18 V. Most of the frequency tuning occurred for charge carrier depletion beneath the grating electrodes with grating bias voltages between −2 to −6 V. The remaining small degree of frequency tuning for grating bias voltages more negative than −7 V is attributable to residual charge carrier depletion between grating lines.

The oscillator temperature sensitivity was measured for several dc reverse bias grating voltages between 0 and −15 V. The measurements were made for temperatures from 10 to 50°C. Within the accuracy of the measurement, the linear TCD was found to be +52.8 ppm/°C, essentially independent of grating bias voltage. This value for the linear TCD is in very reasonable agreement with the value of +52 ppm/°C measured for delay line devices.

The oscillator short-term stability (Allan variance) for a

one second gating time was also measured. Measurements were made for several values of grating reverse bias voltage. For the measurements 240 consecutive frequency readings were taken and the Allan variance and standard deviation calculated. Because the GaAs SAW substrate is not a temperature compensated material, there was frequency drift during the time interval (4 min) required for data taking. The sensitivity of the oscillator to temperature drifting was estimated to set a lower limit of about $4\text{–}8\times10^{-9}$ on the measurement of Allan variance. Measured values of about 1×10^{-8} were obtained for the Allan variance, essentially independent of grating bias voltage. The measured values for Allan variance were typically an order of magnitude better than the values found for the standard deviation. This indicates that the measured values of Allan variance were influenced by temperature drift during the measurement. This limitation on achievable short-term stability may be overcome using temperature compensation techniques such as those previously described and presented elsewhere [6], [7].

While the frequency tuning range of the oscillator was relatively modest (80 ppm), a tuning range of up to approximately 400 ppm should be possible with further development of the epitaxial GaAs SAW resonator configuration. The ability to fabricate the external electronic components on the same monolithic GaAs substrate using present GaAs FET and MIC technologies indicates that a totally monolithic, stable VHF/UHF oscillator may be fabricated for application to radar and communication systems.

IV. Signal Processing

SAW devices have advantages for high speed, wide-bandwidth real-time signal processing applications, including: convolution, correlation, Fourier transformation, and both frequency and transversal filtering. The tapped delay line interaction region design used for the monolithic GaAs SAW signal processors described here is readily adapted to transversal filtering, programmable asynchronous correlation, and matched filtering. Time–bandwidth products of 1000 or greater are achievable using a 10-μs long interaction region, which is equivalent to 10^8 complex multiplications/s. It is important to realize that the devices are electronically tap programmable and thus suited for a wide variety of signal processing applications.

The development of a nondegenerate convolver and an asynchronous matched filter or correlator which uses an FET interaction region design are described. The nonlinear mixing process obtained by operating the FET's below pinch off is shown to be more efficient than that found for Schottky-barrier plate convolver designs described previously in the literature [20], [21]. The nondegenerate operation of the convolver uses the natural periodicity of the FET electrodes to detect the generated sum or difference frequency product signal. By segmenting the FET electrodes, a programmable tapped transveral filter, or asynchronous correlator, has also been developed. Unlike previous hybrid tapped delay line processors [22], [23], the acoustic waves propagate within the FET mixers themselves thus interacting directly with the FET potential fields. Direct control of the amplitude as well as phase $(+/-)$ of the mixer output is achieved by electronic control of the magnitude and polarity of the FET dc bias. The milliwatt level power dissipation per tap, high input dynamic range, large tap amplitude control range and low spurious signal levels achieved represent state-of-the-art performance for tap-programmable correlators. The monolithic configurations described, using n/semi-insulating GaAs, are also compatible with further integration of peripheral electronics including CCD devices as reported previously [24].

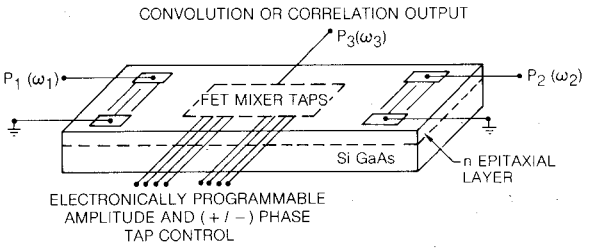

Fig. 7. Basic design of a GaAs SAW convolver or correlator.

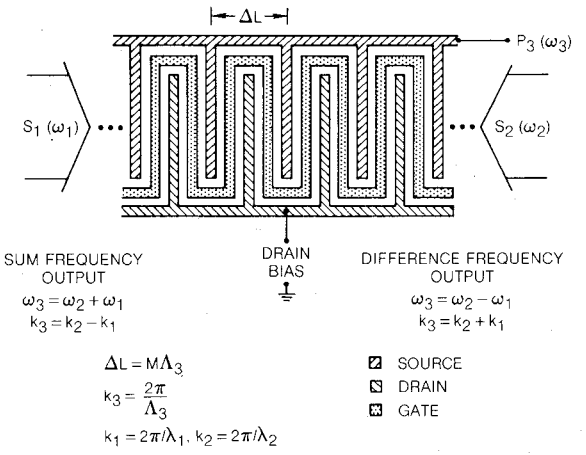

Fig. 8. FET interaction region design for the monolithic GaAs SAW convolver.

A. Convolution Operation

The basic device structure, shown in Fig. 7, may be operated either as a convolver or correlator. For convolver operation, the input and reference coded signals are counter-propagating waves. For this mode of operation, two broad-band input transducers are required at f_1 and f_2, respectively. It is not necessary to segment the interaction region into individual taps, and a uniform bias is applied to the entire interaction region. Fig. 8 shows a schematic representation of the convolver interaction region. Also summarized in Fig. 8 are the equations describing operation with counter-propagating input waves at ω_1 and ω_2, respectively. The basic periodicity of the interaction region is ΔL and the wavevectors $(k_i=2\pi/\lambda_i)$ of the input waves are k_1 and k_2, respectively. Operation with either sum frequency or difference frequency output is indicated along with the appropriate wavevector phase matching condition. Fig. 9(a) shows the nonlinear triangular convolution output

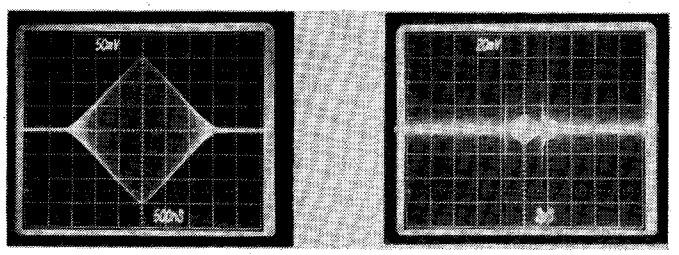

(a) (b)

Fig. 9. Convolver output for 3.2-μs long rectangular input pulses at $f_1 = 106.5$ MHz and $f_2 = 130.8$ MHz. The difference frequency output occurred at $f_3 = 24.3$ MHz. (a) Convolution output, 500 ns/cm. (b) 50-dB double exposure showing post output spurious, 2 μs/cm.

for 3.2-μs long rectangular input signals at $f_1 = 106.5$ MHz and $f_2 = 130.8$ MHz. The difference frequency output occurred at $f_3 = 24.3$ MHz. Fig. 9(b) shows a 50-dB double exposure of the device output in order to estimate the spurious signal level. The spurious signal immediately following the convolution output signal is approximately 50 dB below the peak convolution output signal level.

B. Correlation Operation

The overall configuration of the GaAs monolithic correlator was shown in Fig. 7. For correlation operation, a PSK coded input signal at carrier frequency f_2 is launched at one end of the delay line and interacts with a CW local oscillator wave at frequency f_1 within the central FET-tapped interaction region. Correlation is achieved between the input signal code and the spatial tap code, as electronically programmed through the applied dc bias at each tap. The tap spacing is designed to be equal to the desired input signal chip rate. Because the reference code is electronically programmable at the taps, the device performs as an asynchronous matched filter, with the correlation output at f_3 achieved independent of signal timing and with its time scale unaltered. The input wave at f_1 thus serves only to provide a local oscillator for the mixing process and can be launched by a narrow-bandwidth transducer. The advantages of using a mixing process, rather than a single frequency tapped delay line structure, include the large tap amplitude control range and biphase tap output control provided directly within the FET SAW mixer, and the compensation for acoustic propagation loss through the use of counter-propagating input and local oscillator waves. With the correlation output obtained at a frequency other than the input frequencies or their harmonics, bandpass filtering at the output port eliminates spurious contributions due to direct electromagnetic feedthrough or second harmonic generation.

The FET tap configuration, shown in Fig. 10, consists of segmented Schottky-barrier gate and ohmic contact drain electrodes. The periodicity of the common FET source electrode is chosen to detect the generated sum or difference frequency wavevector produced by the mixing process rather than the waves themselves. The FET periodicity is also consistent with the desired code chip rate which equals the tap sampling frequency, f_s. The experimental correlator had 32 taps with equal linewidths and spacings

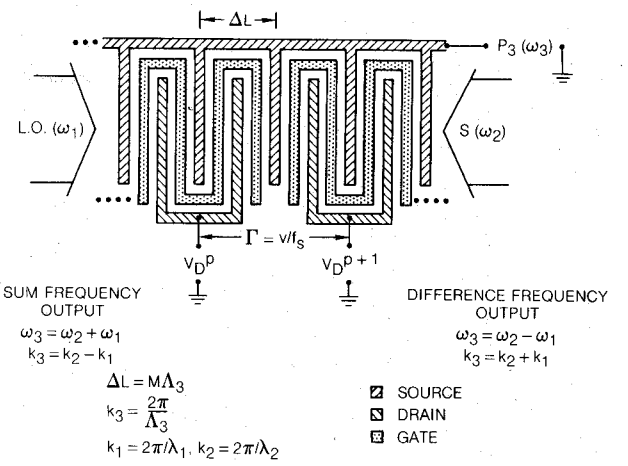

Fig. 10. FET tapped interaction region design for the monolithic, tap programmable GaAs SAW correlator.

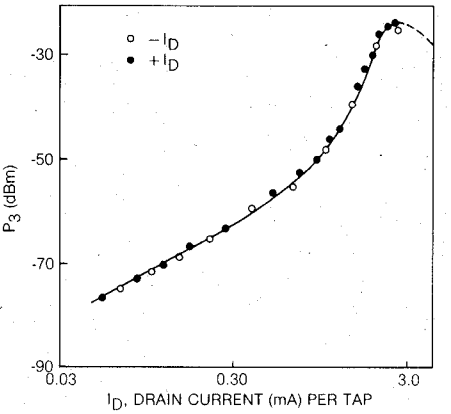

Fig. 11. Nonlinear difference frequency output of tapped FET interaction region as a function of tap dc bias current. $f_1 = 110.56$ MHz, $f_2 = 127.08$ MHz, $P_1 = +22$ dBm, $P_2 = +24$ dBm.

for the source, gate and drain electrodes and an intertap spacing, Γ, of 286.7 μm corresponding to a 10-MHz code chip rate. The epitaxial layer had a carrier concentration of $n = 1 \times 10^{16}/\text{cm}^3$ and a layer thickness of 1.3 μm. Both transducers were of the reverse biased Schottky-barrier type, with 12.5 and 25 wavelengths for the transducers at f_2 and f_1, respectively. The transducers had quarter-wavelength electrodes and 1-mm aperture.

Nominal signal input and local oscillator frequencies of both 130 and 110 MHz were used, and both sum and difference frequency operation were achieved with comparable efficiency. Difference frequency operation was selected because it was found to have better tap weighting properties. Fig. 11 shows the dependence of the difference frequency output on the FET drain current per tap, for equal bias applied to all taps. An amplitude control range of 55 dB is observed, with the same dependence for both positive and negative polarity of the tap bias current. Maximum efficiency is achieved near the FET pinchoff condition and corresponds to a source–drain voltage near 1.5 V. The average power dissipation per tap is 4.5 mW, and ranges from 0.5 to 6 mW over the 32 taps. By reversing the polarity of the drain bias, the phase of the difference

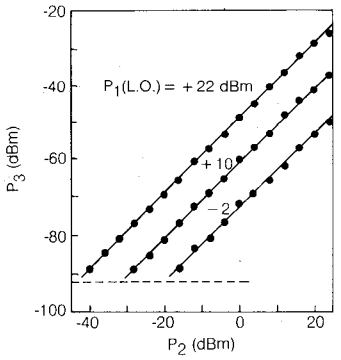

Fig. 12. Nonlinear difference frequency output of tapped FET interaction region as a function of input signal power, for several fixed reference power levels. $f_1 = 110.56$ MHz, $f_2 = 127.08$ MHz.

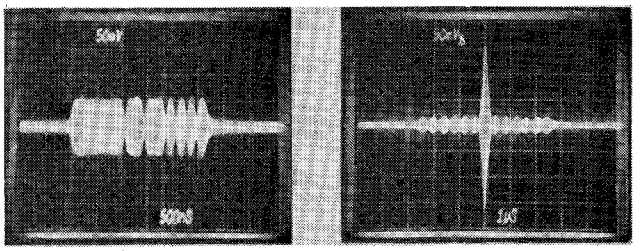

(a) (b)

Fig. 13. Correlation of a 13-chip Barker code with a 5-MHz chip rate. (a) Tap code readout, 500 ns/cm. (b) Difference frequency correlation output at $f_3 = 17.52$ MHz, 1 μs/cm. $f_1 = 110.06$ MHz, $f_2 = 127.58$ MHz, $P_1 = +22$ dBm, $P_2 = +12$ dBm.

frequency tap output is also reversed, permitting biphase code processing. Tap switching speed, measured by reversing the drain current polarity, was near 200 ns, limited by the external circuit capacitance.

The output power versus signal input power is plotted in Fig. 12 for several local oscillator power levels. The P_3 versus P_2 dependence is linear, without evidence of saturation. The external figure of merit, $F_{ext} = P_3/P_1P_2 = -70$ dBm and an input dynamic range exceeding 65 dB were achieved in spite of the approximately 34-dB total insertion loss for the two SAW transducers. Suppression of all spurious signals by 50 dB was also achieved. Measurement of the combined transducer and propagation losses using identical sets of transducers at each end of the correlator resulted in a value for the internal efficiency of $F_{int} = -36.5$ dBm. With further optimization, F_{ext} and F_{int} can be improved considerably.

Fig. 13(a) shows the equalized tap code readout (using external adjustment of individual bias currents), while Fig. 13(b) shows the correlation output waveform for a 13-chip biphase Barker code input sequence, matching the equal amplitude, biphase tap weights. Twenty six taps were biased "on" with two taps per code chip corresponding to a 5-MHz chip rate. The correlation response has near ideal sidelobe response, and a peak to maximum sidelobe ratio of 21 dB.

Fig. 14(a) shows the equalized tap code readout (using external adjustment of individual tap bias currents), while Fig. 14(b) shows the correlation output waveform for a 31-chip pseudorandom M sequence at 10-MHz chip rate.

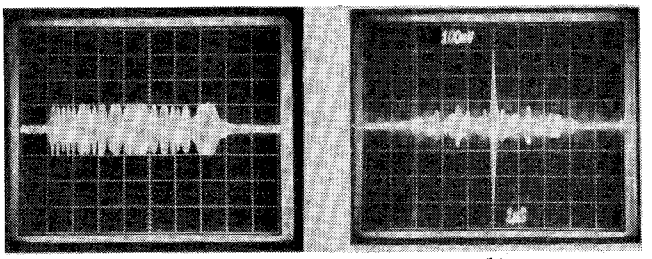

(a) (b)

Fig. 14. Correlation of a 31-chip M sequence code with 10-MHz chip rate. (a) Tap code readout, 500 ns/cm. (b) Difference frequency correlation output at $f_3 = 15.69$ MHz, 1 μs/cm. $f_1 = 110.96$ MHz, $f_2 = 126.65$ MHz, $P_1 = +22$ dBm, $P_2 = +14$ dBm.

The sidelobe distribution is close to the theoretical response for this sequence with a 14-dB sidelobe level compared to the ideal 15.8-dB level [25]. The measured 9.5-MHz bandwidth of the input transducer produced some distortion in the output waveform which could be eliminated by improving the input transducer design or increasing its center frequency.

Epitaxial layer nonuniformity will also contribute to less than ideal correlator performance. These limitations are not fundamental, and further improvements in GaAs epitaxial growth technology will reduce this source of error. Also, in applications such as adaptive filtering, tap uniformity is not a problem because individual tap weighting is performed in an iterative manner.

V. Conclusions

The results demonstrated for monolithic GaAs SAW devices are quite encouraging and show considerable promise for improvement. Device configurations have been pursued which use the same type of fabrication processes and material as are currently being developed for GaAs IC electronics. When moderate bandwidths are needed, only two photomask steps are required for device fabrication and the need for special transducer techniques is eliminated, thus easing fabrication complexity and improving yield. If required, broader bandwidth transducer methods are possible using ZnO or edge-bonded structures.

Several extensions of this monolithic GaAs technology have been shown to be feasible, including charge storage [26], optical imaging [27], and acoustooptic interactions [28]. As the material quality and availability continues to improve, the device performance and application areas have greater potential for further development.

References

[1] R. S. Pengelly, "Monolithic GaAs ICs tackle analog tasks," *Microwaves*, vol. 18, no. 7, pp. 56–65, July 1979.

[2] I. Deyhimy, R. C. Eden, R. J. Anderson, and J. S. Harris, Jr., "A 500 MHz GaAs charge coupled device," *Appl. Phys. Lett.*, vol. 36, no. 2, pp. 151–153, Jan. 15, 1980.

[3] R. Zucca, B. M. Welch, R. C. Eden, and S. I. Long, "GaAs digital IC technology/statistical analysis of device performance," *IEEE Trans. Electron Devices*, vol. ED-27, pp. 1109–1115, June 1980.

[4] T. W. Grudkowski, G. K. Montress, M. Gilden, and J. F. Black, "GaAs monolithic SAW devices for signal processing and frequency control," in *IEEE Ultrasonic Symp. Proc.*, IEEE Cat. 80CH1602-2, vol. 1, pp. 88–97, Nov. 1980.

[5] A. J. Slobodnik, Jr., "GaAs acoustic-surface-wave propagation losses at 1 GHz," *Electron. Lett.*, vol. 8, pp. 307–309, June 15, 1972.
[6] T. W. Grudkowski and M. Gilden, "Realization of temperature-compensated GaAs surface acoustic wave delay lines," *Appl. Phys. Lett.*, vol. 38, no. 6, pp. 412–413, Mar. 15, 1981.
[7] G. Cambon, J. M. Saurel, J. Lassale, J. Attal, and W. Shahab, "Design of temperature stable gallium arsenide surface acoustic wave delay line," *IEEE Trans. Sonics Ultrason.*, vol. SU-28, pp. 106–108, Mar. 1981.
[8] W. R. Smith, H. M. Gerard, J. H. Collins, T. M. Reeder, and H. J. Shaw, "Design of surface wave delay lines with interdigital transducers," *IEEE Trans. Microwave Theory Tech.*, vol. MTT-17, pp. 865–873, Nov. 1969.
[9] G. L. Matthaei, D. Y. Wong, and B. P. O'Shaughnessy, "Simplifications for the Analysis of Interdigital Surface-Wave Devices," *IEEE Trans. Sonics Ultrason.*, vol. SU-22, pp. 105–114, Mar. 1975.
[10] G. S. Kino and R. S. Wagers, "Theory of interdigital couplers on Nonpiezoelectric substrates," *J. Appl. Phys.*, vol. 44, no. 4, pp. 1480–1488, Apr. 1973.
[11] D. C. Webb and C. Banks, "Surface-acoustic-wave excitation in the zinc oxide-on-silicon configuration," in *IEEE Ultrasonics Symp. Proc.*, IEEE Cat. 78CH1344-1SU, pp. 697–700, Sept. 1978.
[12] C. Lardat and P. Defranould, "Application of edge-bonded transducers to SAW components," *Proc. IEEE*, vol. 64, pp. 627–630, May 1976.
[13] J. E. Bowers, B. T. Khuri-Yakub, G. S. Kino, and K-H Yu, "Design and application of high efficiency wideband SAW edge-bonded transducers," in *IEEE Ultrasonics Symp. Proc.*, IEEE Cat. 78CH1344-1SU, pp. 744–748, Sept. 1978.
[14] D. E. Oates and R. A. Becker, "$LiNbO_3$ surface-acoustic-wave edge-bonded transducers on ST quartz and ⟨001⟩-cut GaAs," in *IEEE Ultrasonics Symp. Proc.*, IEEE Cat. 80CH1602-2, vol. 1, pp. 367–370, Nov. 1980.
[15] T. W. Grudkowski, "Active acoustic waves and electrons in gallium arsenide," M. L. rep. 2440, W. W. Hansen Laboratories of Physics, Stanford Univ., Stanford, CA, May 1975, (Ph.D. dissertation).
[16] W. J. Tanski, "Developments in resonators on quartz," in *IEEE Ultrasonics Symp. Proc.*, IEEE Cat. 77CH1264-1SU, pp. 900–904, Oct. 1977.
[17] W. J. Tanski, "Surface acoustic wave resonators on quartz," *IEEE Trans. Sonics Ultrason.*, vol. SU-26, pp. 93–104, Mar. 1979.
[18] D. A. Daly, S. P. Knight, M. Caulton, and R. Ekholdt, "Lumped elements in microwave integrated circuits," *IEEE Trans. Microwave Theory Tech.*, vol. MTT-15, pp. 713–721, Dec. 1967.
[19] W. H. Haydl, P. Hiesinger, R. S. Smith, B. Dischler, and K. Heber, "Design of quartz and lithium niobate SAW resonators using aluminum metallization," in *Proc. 30th Ann. Symp. on Frequency Control*, U. S. Army Electronics Command, Fort Monmouth, NJ, pp. 346–357, 1976. (Copies available from Electronics Industries Association, 2001 Eye Street, NW, Washington, DC 20006.)
[20] G. S. Kino, "Acoustoelectric interactions in acoustic-surface-wave devices," *Proc. IEEE*, vol. 64, pp. 724–748, May 1976.
[21] G. S. Kino, S. Ludvik, H. J. Shaw, W. R. Shreve, J. M. White, and D. K. Winslow, "Signal processing by parametric interactions in delay line devices," *IEEE Trans. Microwave Theory Tech.*, vol. MTT-21, pp. 244–255, Apr. 1973.
[22] T. W. Grudkowski and T. M. Reeder, "Programmable P. S. K. diode convolver," *Electron. Lett.*, vol. 12, no. 8, pp. 186–187, Apr. 15, 1976.
[23] T. M. Reeder and M. Gilden, "Convolution and correlation by nonlinear interaction in a diode-coupled tapped delay line," *Appl. Phys. Lett.*, vol. 22, no. 1, pp. 8–10, Jan. 1, 1973.
[24] D. L. Smythe and R. W. Ralston, "An improved SAW time-integrating correlator with CCD readout," in *IEEE Ultrasonics Symp. Proc.*, IEEE Cat. 80CH1602-2, vol. 1, pp. 14–17, Nov. 1980.
[25] P. H. Carr, P. A. DeVito and T. L. Szabo, "The effect of temperature and Doppler shift on the performance of elastic surface wave encoders and convolvers," *IEEE Trans. Sonics Ultrason.*, vol. SU-19, pp. 357–367, July 1972.
[26] T. W. Grudkowski and C. F. Quate, "Acoustic readout of charge storage on GaAs," *Applied Phys. Lett.*, vol. 25, no. 2, pp. 99–101, July 15, 1974.
[27] T. W. Grudkowski and C. F. Quate, "Optical image scanning using nonlinear surface wave interaction on GaAs," *Ultrasonics Symp. Proc.*, IEEE Cat. 74CH0896-1SU, pp. 749–752, Nov. 1974.
[28] K. W. Loh, W. S. C. Chang, W. R. Smith, and T. W. Grudkowski, "Bragg coupling efficiency for guided acousto-optic interaction in GaAs," *Appl. Opt.*, vol. 15, no. 1, pp. 156–166, Jan. 1976.

Thomas W. Grudkowski (M'75) was born on May 26, 1946. He received the B.S.E.E. degree from the University of Pennsylvania, Philadelphia, in 1968, the M.S. degree in engineering from University of California, Los Angeles, in 1970, and the Ph.D. in electrical engineering from Stanford University, Stanford, CA, in 1975.

From 1968 to 1971, he was a member of the technical staff of Hughes Aircraft Company and worked in the areas of microelectronics and infrared electro-optics at Hughes-Culver City and Malibu Research Labs. He subsequently did his doctoral work at Stanford Ginzton Laboratory in the area of surface and bulk acoustic wave interactions in GaAs. Since joining the staff of the United Technologies Research Center, he has been engaged in microwave acoustic and semiconductor device research for application to signal processing, frequency control, and GaAs technology development. He is currently Manager of the Electronics Research Laboratory of UTRC.

He is a member of Sigma Xi, and Eta Kappa Nu.

✤

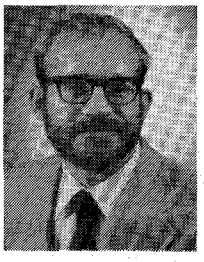

Gary K. Montress (S'66–M'76) was born in East Orange, NJ, on April 10, 1947. He received the B.S.E.E., M.S.E.E., electrical engineer, and Ph.D. degrees from the Massachusetts Institute of Technology, Cambridge, MA, in 1969, 1971, 1971, and 1976, respectively.

From 1969 to 1972, while at the Massachusetts Institute of Technology, he was a Teaching Assistant in the Electrical Engineering Department teaching courses on solid-state electronics and circuit design and pursuing research on *p-n* junction breakdown phenomena. From 1972 to 1975, he was an Instructor in the Electrical Engineering Department, teaching and supervising courses on solid-state device physics and microelectronics. From 1975 to 1976, while a Research Assistant in the Research Laboratory for Electronics, he completed his Ph.D. thesis research and dissertation in the area of Solid-State Microwave Devices. Since September 1976, he has been a member of the Professional Staff at United Technologies Research Center, East Hartford, CT, where he is engaged in research on solid-state electronics, SAW frequency control and signal processing components, and GaAs material and device technologies for SAW and electronic device applications.

Dr. Montress is a member of Eta Kappa Nu, Sigma Xi, and Tau Beta Pi.

✤

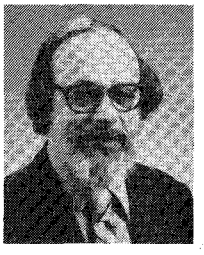

Meyer Gilden (S'47–A'48–M'55) was born in Chicago, IL, in 1924. He received the B.S. and M.S. degrees in electrical engineering from Illinois Institute of Technology, Chicago, in 1946 and 1948, respectively, and the Ph.D. from the University of Illinois, Urbana in 1955.

He is presently at the United Technologies Research Center, which he joined in 1971 and has been in charge of microwave physics programs encompassing the application of microwave concepts to solid-state signal and power sources, surface-acoustic-wave oscillators and other devices, and to microwave optical devices. He held teaching and research positions at Illinois Institute of Technology and then at the University of Illinois and was an Assistant Professor when he left in 1956. His affiliations include the G.E. Microwave Laboratory from 1956 to 1959, Stanford Research Institute from 1959 to 1961, Microwave Associates from 1961 to 1969, and the Monsanto Microwave Products Department from 1969 to 1971. His experience and contributions include work in the areas of SAW oscillators and devices, solid-state microwave power sources, microwave integrated circuits, parametric amplifiers,and microwave gas discharge phenomena and devices.

He is a member of Eta Kappa Nu, and Sigma Xi, and the American Physical Society. His activities in the IEEE include serving as an officer of the Boston Chapter of MTT, a member of the MTT-6 Advisory Group on MIC and a member of several Program Committees for the International MTT Symposium.

James F. Black (M'71) was born in New York City, NY, on January 22, 1927. He received the B.S. degree in chemistry from Polytechnic Institute of Brooklyn, Brooklyn, NY in 1960.

From 1948 to 1972, he was at General Telephone and Electronics Laboratories, and its predecessor Sylvania Research Center, in Bayside, NY, working first on diffusion, precipitation, and recrystallization phenomena, and later specializing in III–V compounds. From 1960 to 1968, he conducted research programs in bulk crystal growth, LED's, diode lasers, materials for IMPATT devices and Hilsum–Gunn diodes, and use of lasers for infrared imaging and photoluminescence imaging. From 1968 to 1972 as Head, Compound Semiconductor Section, he was responsible for programs on liquid and vapor phase epitaxial growth, materials and device characterization, and process control technology. Since 1972, he has been a member of the Professional Staff at United Technologies Research Center, East Hartford, CT, where he has been engaged in silicon and gallium arsenide materials and device programs, including the fields of integrated optics, optoelectronics, microwaves and acoustic waves, and involving such devices as IMPATT's, grating couplers, FET's, LED's for fiber optics, high temperature rectifier diodes, and SAW and BAW filters.

Mr. Black is a member of APS, Electrochemical Society, and Sigma Xi. He has authored/co-authored over twenty technical publications.

A High-Power Dual Six-Port Automatic Network Analyzer Used in Determining Biological Effects of RF and Microwave Radiation

CLETUS A. HOER, MEMBER, IEEE

Abstract—**The design, calibration, and performance of a high-power (1-1000 W) automatic network analyzer based on the six-port concept are described for the 10–100-MHz range. Calibration is performed with a length of transmission line as the only impedence standard needed. A 10-mW thermistor mount is the standard of power. Imprecision in measuring reflection coefficient Γ is 0.0001 in magnitude and $0.005/|\Gamma|$ degrees in phase. Corresponding estimated systematic errors are 0.001 and $0.1/|\Gamma|$ degrees. Imprecision in measuring power is 0.01 percent of range (20 W, 200 W, or 1000 W) with an estimated systematic error of 1.25 percent of reading.**

I. Introduction

IN SPITE OF the existence of so-called "safe tolerance limits" to microwave radiation, there is a continuing interest in obtaining a more complete understanding of this subject. At the National Institute for Occupational Safety and Health (NIOSH), a program exists for evaluating the response of selected biological specimens to carefully measured and controlled electromagnetic fields with the objective of determining safe levels of RF and microwave radiation. The associated test chamber is designed in such a way as to provide fields which are predominantly either electric, magnetic, or selected combinations of both. This test chamber, shown schematically in Fig. 1, is a near-field synthesizer [1] consisting of a balanced, parallel-plate strip line to generate the electric field, and a rotatable single-turn inductor placed parallel to and midway between the plates to generate the magnetic field.

The purpose of this paper is to describe the design, calibration, and performance of a high-power automatic network analyzer (ANA) designed for NIOSH by NBS to measure the power and reflection coefficient at the *E*- and *H*-field input ports of this test chamber at power levels of 1–1000 W and frequencies of 10–100 MHz. Measurements at the inputs to the near-field synthesizer are made with two six-port reflectometers as shown in Fig. 1. The design of the reflectometers is based on the new six-port concept of measurement [2], [3]. Basically, for one six-port the concept states that the power and reflection coefficient at one-port of any linear network having six ports can be obtained from measurements of the power at four other ports when a signal is applied to the remaining port.

Six-port reflectometers were chosen as the measuring instruments in this application because of the following significant features which are not found in other automated measurement systems: 1) *simplicity* of the construction, operation, and calibration; 2) *superior accuracy* and precision; 3) *no lossy standards* required in the calibration; 4) *stability* of the calibration with time.

These features are elaborated on below.

Manuscript received April 13, 1981; revised August 5, 1981. This work was supported in part by the National Institute for Occupational Safety and Health.

The author is with the Electromagnetic Technology Division, National Bureau of Standards, Boulder, CO 80303.